IEICE Electronics Express, Vol.19, No.1, 1–4

LETTER

Comparing distortion and power characteristics of AlGaN/GaN HEMTs between SiC and GaN substrates

Atsushi Moriwaki[1] **and Shinji Hara**[1, a)]

Abstract In this paper, we compare the distortion and power characteristics between AlGaN/GaN high-electron-mobility transistors (HEMTs) with different epi-structures. Third-order intermodulation distortion (IM3) measurement evaluates distortion characteristics, and on-wafer load and source-pull measurements evaluate the power performance. The results show that the AlGaN/GaN HEMTs directly fabricated on GaN substrates without nucleation layer perform better than those fabricated on SiC substrates. Furthermore, the distortion performance is compared with and without field plate.

Keywords: AlGaN/GaN, high-electron-mobility transistor (HEMT), free-standing GaN substrate, SiC substrate, current collapse, intermodulation distortion

Classification: Microwave and millimeter wave devices, circuits, and hardware

1. Introduction

Microwave power amplifiers are key devices that utilize AlGaN/GaN high-electron-mobility transistors (HEMTs) [1, 2, 3, 4, 5, 6, 7, 8, 9, 10, 11, 12, 13]. Amplifier distortion becomes critical because wideband and multivalue linear modulation is used to achieve high speed and large capacity in modern wireless communication. Using the digital predistortion (DPD) algorithm that applies an inverse distortion to the input signal has become a recent trend in reducing the distortion [14, 15, 16, 17, 18]. However, memory effects complicate the algorithm and increase the DPD current consumption; therefore, memory effects should be reduced to achieve highly linear power amplification. The major memory effects of GaN HEMT are thermal transient response and current collapse from electron trapping after bias stress. Thermal memory effects are common for most semiconductor devices. When using GaN HEMT, the current collapse is another critical memory effect to realize a linear power amplifier, and considerable research has been conducted to analyze the phenomena and solve the current collapse of GaN HEMT [1]. The AlGaN/GaN HEMTs fabricated on free-standing GaN substrates exhibit fewer defects than that fabricated on SiC substrates, resulting in fewer traps and lower current collapse [19, 20, 21]. In this paper, the distortion caused by the current collapse is compared between different structures of devices. The distortion restraint by the field plate (FP) [22, 23, 24, 25, 26, 27, 28, 29, 30, 31] is also evaluated. The load-pull measurement is performed to compare the power characteristics. The AlGaN/GaN HEMT on GaN substrates exhibit better power and distortion characteristics compared with AlGaN/GaN HEMT on SiC substrates.

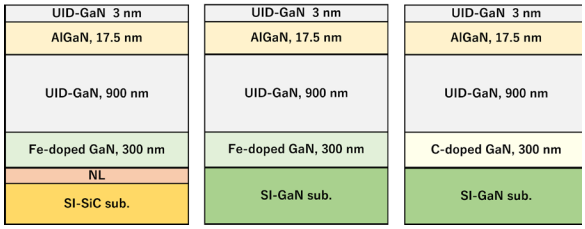

Fig. 1 Schematic wafer structure. (a) GaN(Fe)-on-SiC, (b) GaN(Fe)-on-GaN, and (c) GaN(C)-on-GaN. A nucleation layer (NL) is in (a) but not in (b) and (c).

2. Material

Six types of devices composed of three epi-structures and two types of device structures are compared. Fig. 1 shows schematic epi-structures of the evaluated wafers. We evaluated GaN HEMT fabricated on SiC or GaN substrates. GaN on SiC structures require a nucleation layer between a doping GaN layer and SiC substrate, whereas GaN on GaN structures do not require it. Therefore, we can expect a lower current collapse of GaN on GaN compared with GaN on SiC owing to lower defects. For GaN on GaN structures, two types of doping, iron (Fe) and carbon (C), were applied to the buffer layer. As described, three epi-structures are used in this paper, namely, GaN(Fe)-on-SiC, GaN(Fe)-on-GaN, and GaN(C)-on-GaN.

Each wafer has two device structures, i.e., with and without the FP. The FP structure is commonly used to reduce the current collapse in GaN HEMT. The identical HEMT, except the FP, with a gate length of 1 um and width of 100 um*2, was fabricated on each epi-structure.

3. Distortion measurement setups

The third-order intermodulation distortions (IM3) were evaluated to compare the current collapse of GaN HEMT distortion performance because IM3 is the basic performance parameter to evaluate device distortion. IM3 results from the nonlinearity of the transconductance [32]. When there is any feedback loop from the drain to the gate that cannot

[1] Institute of Materials and Systems for Sustainability, NAGOYA University, Furo-cho, Chikusa-ku, Nagoya 464-8601, Japan. (A. Moriwaki is now retired.)

[a)] shinjihara@imass.nagoya-u.ac.jp

DOI: 10.1587/elex.18.20210486
Received November 15, 2021
Accepted November 22, 2021
Publicized November 30, 2021
Copyedited January 10, 2022

be neglected in the microwave region, IM3 also comes from mixing fundamental wave and second-order intermodulation distortion (IM2). The current collapse changes the low frequency impedance; thus, the IM2 performance changes with the current collapse level. Therefore, six devices must show different IM3 performances.

Two IM3 measurements were performed which had different impedance at low frequency region. One had very low impedance, ideally short, that is a conventional IM3 measurement. The other had 1 kΩ which was realized by using diplexer with a 1-kΩ series resistor instead of bias-T at the drain side.

The following conditions were used in the conventional IM3 measurement.

- The center frequency, $fc = (f1 + f2)/2$, is 1 and 2.4 GHz.
- The spacing frequency, $\Delta f = f2 - f1$, is one point per decade from 20 Hz to 20 MHz.
- The bias condition is 20-V Vds and the quiescent current, Idq, is 3.32 and 15 mA, which are deep and shallow class AB bias points.

In 1-kΩ load at Δf measurement setup, the following conditions were used.

- fc is only 1 GHz.
- Δf is the same as the conventional IM3 measurement.
- Vds is lowered from 20 to 10 V to increase the sensitivity to Ron, and the Idq is only 3.32 mA.

4. Measurement results

Before comparing the distortion, the basic DC and small-signal RF performances were compared, and all six devices confirmed to perform similarly. Fig. 2 shows the IM3 measurement result from the conventional IM3 measurement as a function of the output power (Pout) of a single tone wave. The plots are for $fc = 2.4$ GHz, $\Delta f = 2$ MHz. Fig. 2(b), the shallow class AB that in the linear bias region, shows GaN-on-GaN HEMTs have smaller distortions than GaN-on-SiC HEMT, and GaN(C)-on-GaN has smaller distortions than GaN(Fe)-on-GaN. These observations were common with both $fc = 1.0$ GHz and $fc = 2.4$ GHz across all Δf's.

The nonlinearity of the transconductance, gm, is evaluated to determine whether the IM3 difference is because of it or the current collapse. Fig. 3 compares gm performances between devices from three epi-structures. For the second derivative of gm, GaN(C)-on-GaN is the largest, followed by GaN(Fe)-on-GaN and GaN(Fe)-on-SiC. If gm results in the difference in IM3, IM3 will decrease in the same order in which the second derivative of gm decreases. However, the IM3 decreases in the order: GaN-on-SiC, GaN(Fe)-on-GaN, and GaN(C)-on-GaN, which is the reverse of that given above. Therefore, this IM3 result does not originate from the nonlinearity of gm but the current collapse.

Fig. 4 shows the IM3 measurement result from 1-kΩ load measurement as a function of Pout of a single tone wave. Fig. 4(a) compares IM3 of HEMTs that do not have an FP. The GaN-on-GaN HEMTs exhibit lower distortion than GaN-on-SiC HEMTs. GaN(C)-on-GaN shows slightly lower distortion than GaN(Fe)-on-GaN. This result is the same as that given in Fig. 2. Fig. 4(b) and (c) are the IM3 performances of HEMTs that have FPs. In Fig. 4(b), the IM3 of each HEMT improves from Fig. 4(a), and the improvement amount of GaN-on-SiC HEMT is larger than that of GaN-on-GaN HEMT. Therefore, the superiority of GaN(Fe)-on-GaN to GaN(Fe)-on-SiC HEMT is unclear. In Fig. 4(c), the stress voltage increases to 15 V. The IM3 difference between GaN-on-GaN and GaN-on-SiC and the superiority of GaN-on-GaN become clear.

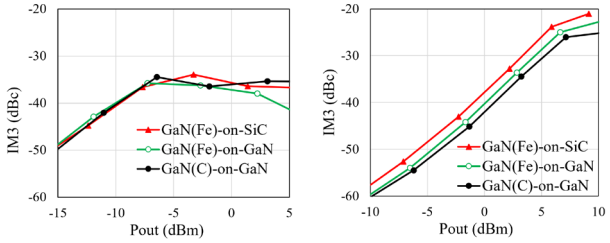

(a) Idq=3.32mA (b) Idq=15mA

Fig. 2 IM3 of HEMT with FP as a function of Pout.

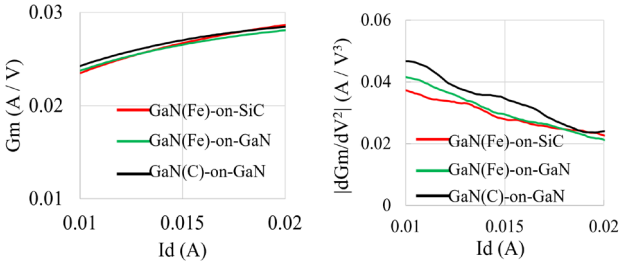

(a) Transconductance, Gm (b) Second deviative of Gm

Fig. 3 Transconductance of HEMT with FP as a function of Id.

As the summary of IM3 measurement,

- the GaN-on-GaN structure exhibits better linearity than GaN-on-SiC.
- by using FP, the linearity improves and the difference between the epi-structure decreases.
- the superiority of the GaN-on-GaN linearity is remarkable under a higher operating voltage.

5. Power performance

The power characteristics of the HEMT with FPs are evaluated using on-wafer load and source-pull systems. The impedances were tuned to maximize the power-added efficiency. Fig. 5 shows the results of the gain, output power (Pout), drain efficiency (ηD), and power-added efficiency (PAE) as functions of the input power (Pin) at 2.4 GHz. The bias condition is Vds = 20 V and Idq = 3 mA. GaN(C)-on-GaN is the best for the power characteristics followed by GaN(Fe)-on-GaN and G aN(Fe)-on-SiC, which is of the same order as the distortion characteristics.

6. Conclusion

The distortion and power characteristics of AlGaN/GaN HEMTs are compared with different epi-structures. Both characteristics show that GaN-on-GaN devices are superior to GaN-on-SiC devices. The distortion of GaN-on-SiC

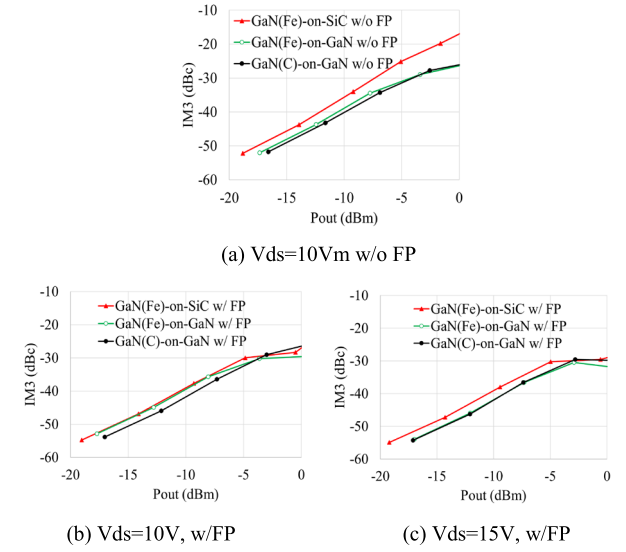

(a) Vds=10Vm w/o FP

(b) Vds=10V, w/FP (c) Vds=15V, w/FP

Fig. 4 IM3 as a function of Pout measured with fc = 1 GHz and Δf = 200 kHz.

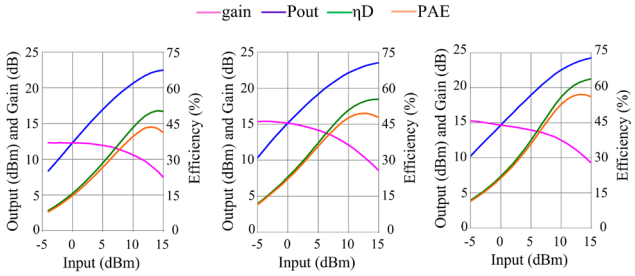

(a) GaN(Fe)-on-SiC (b) GaN(Fe)-on-GaN (c) GaN(C)-on-GaN

Fig. 5 Comparison of power characteristics between wafers.

HEMTs can be reduced by adding a FP structure but cannot be reduced to be as small as that of GaN-on-GaN HEMTs. The superiority of GaN-on-GaN HEMTs comes from a lower current collapse owing to the fewer GaN-on-GaN structure traps. GaN-on-GaN HEMTs will not only maximize the merit of the high-power capability of GaN HEMT but also realize better linearity compared with GaN-on-SiC HEMT.

Acknowledgments

The authors would like to thank Mitsubishi Electric Corp. Advanced Technology R&D Center for their supply of the devices and Prof. A. Wakejima from Nagoya Institute of Technology for his support of load pull measurement.

This work was supported by MEXT "Research and development of next-generation semiconductor to realize energy-saving society" Program Grant Number JPJ005357.

References

[1] Y. Hao, *et al.*: "Research on GaN-based RF devices," Microwave Mag. **22** (2021) 34 (DOI: 10.1109/MMM.2020.3047746).
[2] A. Grebennikov, *et al.*: "High-power high-efficiency GaN HEMT Doherty amplifiers for base station applications," IEICE Trans. Electron., **E104-C** (2021) 488 (DOI: 10.1587/transele.2021MMI0003).
[3] U.K. Mishra, *et al.*: "GaN-based RF power devices and amplifiers," Proc. IEEE **96** (2008) 287 (DOI: 10.1109/JPROC.2007.911060).
[4] R.S. Pengelly, *et al.*: "A review of GaN on SiC high electron-mobility power transistors and MMICs," IEEE Trans. Microw. Theory Techn. **60** (2012) 1764 (DOI: 10.1109/TMTT.2012.2187535).
[5] P. Wright, *et al.*: "A methodology for realizing high efficiency class-J in a linear and broadband PA," IEEE Trans. Microw. Theory Techn. **57** (2009) 3196 (DOI: 10.1109/TMTT.2009.2033295).
[6] K. Chen, *et al.*: "Design of highly efficient broadband class-E power amplifier using synthesized low-pass matching networks," IEEE Trans. Microw. Theory Techn. **59** (2011) 3162 (DOI: 10.1109/TMTT.2011.2169080).
[7] N. Tuffy, *et al.*: "A simplified broadband design methodology for linearized high-efficiency continuous class-F power amplifiers," IEEE Trans. Microw. Theory Techn. **60** (2012) 1952 (DOI: 10.1109/TMTT.2012.2187534).
[8] M.J. Pelk, *et al.*: "A high-efficiency 100-W GaN three-way Doherty amplifier for base-station applications," IEEE Trans. Microw. Theory Techn. **56** (2008) 1582 (DOI: 10.1109/TMTT.2008.924364).
[9] S. Zhou, *et al.*: "Characteristics modeling of GaN class-AB dual-band PA under different temperature and humidity conditions," IEEE Access **9** (2021) 121632 (DOI: 10.1109/ACCESS.2021.3108583).
[10] W. Shi, *et al.*: "Design of a C-band high efficiency power amplifier with compact harmonic control network," IEEE Microw. Wireless Compon. Lett. **31** (2021) 1059 (DOI: 10.1109/LMWC.2021.3096251).
[11] G. Formicone, *et al.*: "A study for achieving high power and efficiency based on high bias operation in C- and X-band GaN power amplifiers," 2018 IEEE Topical Conference on RF/Microwave Power Amplifiers for Radio and Wireless Applications (2018) 39 (DOI: 10.1109/PAWR.2018.8310062).
[12] J. Wong, *et al.*: "High-power high-efficiency broadband GaN HEMT Doherty amplifiers for base station applications," 2018 IEEE Topical Conference on RF/Microwave Power Amplifiers for Radio and Wireless Applications (2018) 16 (DOI: 10.1109/PAWR.2018.8310055).
[13] J. Kim, *et al.*: "A high-performance GaN-modified nonuniform distributed power amplifier," IEEE Trans. Microw. Theory Techn. **68** (2020) 1729 (DOI: 10.1109/TMTT.2020.2972277).
[14] J. Wood: "System-level design considerations for digital predistortion of wireless base station transmitters," IEEE Trans. Microw. Theory Techn. **65** (2017) 1880 (DOI: 1109/TMTT.2017.2659738).
[15] S. Kimura, *et al.*: "How to design an outphasing power amplifier with digital predistortion," IEICE Trans. Electron. **E104-C** (2021) 472 (DOI: 10.1587/transele.2021MMI0006).
[16] S. Wang, *et al.*: "Infinite impulse response structure for amplifier modeling and linearization," IEEE Microw. Wireless Componen. Lett. **31** (2021) 961 (DOI: 10.1109/LMWC.2021.3088255).
[17] L. Chen, *et al.*: "A robust and scalable harmonic cancellation digital predistortion technique for HF transmitters," IEEE Trans. Microw. Theory Techn. **68** (2020) 2796 (DOI: 10.1109/TMTT.2020.2979438).
[18] A. Katz, *et al.*: "The evolution of PA linearization: from classic feedforward and feedback through analog and digital predistortion," IEEE Microw. Mag. **17** (2016) 32 (DOI: 1109/MMM.2015.2498079).
[19] Q. Ma, *et al.*: "Dynamic characteristics after bias stress of GaN HEMTs with field plate on free-standing GaN substrate," Electronics Lett. **57** (2021) 591 (DOI: 10.1049/ell2.12201).
[20] Y. Kumazaki, *et al.*: "Remarkable current collapse suppression in GaN HEMTs on free-standing GaN substrates," 2019 IEEE BiCMOS and Compound Semiconductor Integrated Circuits and Technology Symposium (BCICTS) (2019) (DOI: 10.1109/BCICTS45179.2019.8972742).
[21] T.J. Anderson, *et al.*: "Effect of reduced extended defect density in MOCVD grown AlGaN/GaN HEMTs on native GaN substrates," IEEE Electron Device Lett. **37** (2016) 28 (DOI: 10.1109/LED.2015.2502221).
[22] K. Lee, *et al.*: "Improved DC and RF performance of high power AlGaN/GaN HEMTs with a novel inner field-plate," IEEE 2006 Asia-Pacific Microwave Conference (2006) 1019 (DOI: 10.1109/APMC.2006.4429583).
[23] B. Benbakhti, *et al.*: "Study of field plate AlGaN/GaN HEMTs by means of a 2D-hydrdynamic model for power applications," IEEE 2006 European Microwave Integrated Circuits Conference (2006) 363 (DOI: 10.1109/EMICC.2006.282657).
[24] V. Adivarahan, *et al.*: "Stable CW operation of field-plated GaN-

AlGaN MOSHFETs at 19 W/mm," IEEE Electron Device Lett. **26** (2005) 535 (DOI: 10.1109/LED.2005.852740).

[25] D. Godfrey, *et al.*: "Investigation of AlGaN/GaN HEMT breakdown analysis with source field plate length for high power applications," IEEE 2020 5th International Conference on Device, Circuits and Systems (ICDCS) (2020) 244 (DOI: 10.1109/ICDCS48716.2020.243589).

[26] A. Toprak, *et al.*: "Effect of gate field plate and Γ(gamma)-gate structures on RF power performance of AlGaN/GaN HEMTs," IEEE 2015 10th European Microwave Integrated Circuits Conference (EuMIC) (2015) 215 (DOI: 10.1109/EuMIC.2015.7345107).

[27] Y.-F. Wu, *et al.*: "30-W/mm GaN HEMTs by field plate optimization," IEEE Electron Device Lett. **25** (2004) 117 (DOI: 10.1109/LED.2003.822667).

[28] L. Weijun, *et al.*: "Structure optimization of field-plate AlGaN/GaN HEMTs," 2006 8th International Conference on Solid-State and Integrated Circuits Technology Proceedings (2006) 926 (DOI: 10.1109/ICSICT.2006.306596).

[29] M.T. Hasan, *et al.*: "Current collapse suppression by gate field-plate in AlGaN/GaN HEMTs," IEEE Electron Device Lett. **34** (2013) 1379 (DOI: 10.1109/LED.2013.2280712).

[30] A. Koudymov, *et al.*: "Mechanism of current collapse removal in field-plated nitride HFETs," IEEE Electron Device Lett. **26** (2005) 704 (DOI: 10.1109/LED.2005.855409).

[31] Q. Ma, *et al.*: "Transient response of drain current following biasing stress in GaN HEMTs on SiC substrates with a field plate," Jpn. J. Appl. Phys. **59** (2020) 101002 (DOI: 10.35848/1347-4065/abb7e2).

[32] R.A. Minasian: "Intermodulation distortion analysis of MESFET amplifiers using the volterra series representation," IEEE Trans. Microw. Theory Techn. **28** (1980) 1 (DOI: 10.1109/TMTT. 1980.1129998).